

Active and Passive disturbance isolation for high accuracy control systems

Fabrice Boquet, Alexandre Falcoz, Jean-Pascal Lejault, Samir Bennani

Abstract Micro-vibrations are a major contributor to the performances of an increasing number of Earth Observation and space science missions as line of sight stability requirements get tighter with increasing resolution and longer instruments integration time. These mission performances are sensitive to the presence of disturbance sources such as wheels, cryocoolers and solar array drive mechanisms. Astrium is currently managing microvibrations attenuation by implementing elastomer-based isolators set at the reaction wheels interface without locking devices. This flight-proven passive solution guarantees good rejection performances at high frequencies in line with current mission requirements. However, such systems cannot offer by nature high isolation capability at low frequencies, which could reveal insufficient for future demanding Earth and Science Observation programmes. This paper presents the work done in the frame of an ESA study on the design of mixed passive and active solutions offering extended insulation performances over a large frequency band. The preferred solution is based on a passive isolator coupled with an active control system in charge of rejecting disturbances in the low frequency band. Two kinds of active controllers have been designed and implemented. The first one is based on an adaptive disturbance cancellation scheme operating in the output demodulated space while the second one is formulated and managed in the H_∞/μ setting. The plant model, used for the controllers design procedure, has been derived from a prior ARMAX-type MIMO identification procedure considering input/output experimental time measurements collected on the real system. The two control solutions have been implemented on a dedicated hardware test bench facility and a robust performances assessment campaign has been performed demonstrating more than 20dB disturbance rejection even on a partially modeled structure.

Fabrice Boquet, Alexandre Falcoz
Astrium Satellites, 31405 Toulouse Cedex, France,
fabrice.boquet@astrium.eads.net, alexandre.falcoz@astrium.eads.net

Jean-Pascal Lejault, Samir Bennani
European Space Agency, Keplerlaan 1, 2201 AZ Noordwijk, The Netherlands,
Jean-Pascal.Lejault@esa.int, Samir.Bennani@esa.int

2

Table of Contents

Active and Passive disturbance isolation for high accuracy control systems... 1	
1 Introduction..... 3	
2 Performance requirements..... 5	
3 Active /Passive Solution and Test Set-Up Description 7	
3.1 Active Isolation System..... 7	
3.2 Test Set-Up description 8	
3.3 Structure Identification 9	
4 Active Control Laws..... 10	
4.1 Anti-Phase Cancellation 10	
4.2 Robust control design 11	
4.3 Gain-scheduling control..... 12	
5 Performances with Hardware in the Loop 13	
5.1 Steady-state nominal performances..... 14	
5.2 Steady-state robust performances..... 15	
5.3 Time-varying performances 16	
6 Study conclusions and way-forward..... 17	

1 Introduction

Abstract Microvibrations are a major contributor to observation and science missions pointing stability performances. For a majority of Astrium satellites, microvibration mitigation is handled by passive isolators performing a good high frequency disturbances rejection. The use of active control in conjunction with passive isolation complements this rejection in the low frequency band thus improving the global pointing stability performances. For missions needing a very high platform stability, this solution could enable the use of standard reaction wheels during the critical phases of the mission, which then would prevent from implementing a specific vibration-free propulsion system specifically for these phases. A unique reaction wheels system with mixed passive and active isolators could then reveal of great interest in terms of cost, mass, and operational simplicity with the possibility to use the wheels during all mission phases. This research activity led by Astrium Satellites and the European Space Agency has investigated the design of a hybrid active/passive control strategy for multi-harmonic microvibrations mitigation, and evaluated its performances on a hardware breadboard developed in the frame of this study.

Microvibrations on-board observation and science spacecrafts are becoming a major contributor to their pointing stability performances due to more and more stringent system requirements. Any on-board equipment that includes one or several mobile parts shall then be considered as a potential source of microvibrations. This includes bus equipments such as reaction wheels, gyros, infrared-earth sensors, solar array drive mechanisms, thrusters, or payload elements such as pointing mechanisms, cryocoolers, RF switches or scan mechanisms. The most critical sources are reaction wheels that generate multi-frequency and time-varying harmonic disturbances due to the interaction of wheel unbalance and ball-bearing flaws with spacecraft structure modes. Sources like cryocooler or solar array drive mechanisms generate also significant harmonics disturbances but at constant frequencies. Then coincidence with satellite structure modes can be avoided by stiffening or softening the structure and/or by tuning the source fundamental frequency (e.g. wheel rate in a Control Momentum Gyro) and/or by specific harmonic active control (cryocoolers).

Microvibration mitigation can be handled by passive isolators set either at the base of the main disturbance sources, usually the wheels, or between the platform and the payload. A combination of both configuration is also possible (double-stage system) thus improving filtering function. Passive isolation systems developed by Astrium Satellites and flying onboard operational high resolution Earth Observation systems are very light-weight elastomer-based isolators able to withstand launch loads without requiring a locking device and testable under 1-g. Such

passive isolators are roughly comparable to a second order low pass filter with a resonance frequency f_0 thus rejecting disturbances with frequencies far above f_0 . Disturbances with frequencies below f_0 are not rejected, and disturbances in the vicinity of f_0 are amplified by the Q-factor of the isolator. An advantage of elastomer-based passive isolators with respect to metallic ones is that Q-factor is then limited to about 3 to 4 due to the natural damping of elastomeric materials.

However, for missions requiring very high pointing stability in a wide frequency band (like GAIA or LISA PATHFINDER), such passive isolation may reveal even insufficient to meet the mission pointing requirements when using wheels. The solution then consists in replacing the wheels by more expensive, massive and complex micro-propulsion system. In this context, active strategy for micro-vibration mitigation is an attractive alternative to mitigate micro-vibrations in a larger frequency range and to provide performances that could rival with micro-propulsion while allowing the use of wheels during mission phases.

Mixed Active/Passive isolation systems have been studied by a great number of authors in the past decade and Astrium Satellites has been working with ESA on different projects related to microvibration active damping and isolation.

The work presented in this document results from another TRP research activity led by Astrium Satellites and the European Space Agency on the design of an optimized hybrid solution combining a passive isolator and an active controller in order to limit the microvibrations transmitted at the base of a wheel towards the satellite structure. Passive isolator is in charge of rejecting high frequency disturbances, whereas active control rejects disturbances in the low frequency band and, in particular in the vicinity of the isolator resonance frequency with an objective of 20dB attenuation above 10Hz. Two controllers have been designed and implemented: the first one, called anti-phase controller, is based on an adaptive feed-forward disturbance cancellation scheme; the second one is formulated in the μ -synthesis framework to handle robust stability and performances specifications. The model of the plant, including the sensors and the actuators is based on an ARMAX-type MIMO identification procedure. The performances of the solution have been evaluated in real-time on a hardware test bench also developed in the frame of this study.

2 Performance requirements

Abstract Different missions sensitive to microvibration have been analysed and the most critical ones identified and used to assess disturbance rejection performance requirements. Images are very sensitive to micro-vibrations especially for frequencies above 0.1 times the image acquisition frequency creating non rectifiable image blurring. For missions requiring a very long integration time or for very high resolution missions, passive isolation may be too limited at low frequencies. The use of active control as a complement to passive isolation in the lower frequency band can then allow reaching the desired performances.

Microvibrations degrade the image in two ways: “high frequency” disturbances degrade the Modulation Transfer Function (MTF) inducing image blurring, whereas “lower frequency” ones degrade the geometry inducing image distortions. In some cases, image distortions can be corrected on-ground by dedicated algorithms, but image blurring is definitely not rectifiable. This high/low frequency limit separation depends on the integration time: it is usually roughly equal to 0.1 times the inverse of the integration time. Hence, long integration time instruments like the ones used in scientific missions are more affected by MTF degradation than short integration time ones as in LEO Earth observation missions.

During this study, different Earth observation, interplanetary and science missions have been analyzed in terms of stability requirements and on-board equipment likely to generate microvibration disturbances during the mission phase.

The different missions used for this analysis are summarized in the next table

Satellite	Mission	Stability (μ rad)	Integration Time	Disturbances sources
MTG	GEO Earth Observation	1	100ms	4 wheels 1 cryocooler SADM
Geo-oculus	GEO Earth Observation	0,15	100ms	4 wheels 1 cryocooler
IXO	Science : X observation	4,8	100ms	5 wheels at least 1 cryocooler
Plato	Science : exoplanets and their stars observation	0,1	14h	No wheels in baseline No cryocooler

The most challenging mission is Geo-Oculus (an Earth Observation mission in GEO); Geo-Oculus uses 4 wheels and a cryocooler and has a pointing stability of $0.15\mu\text{rad}$ during 100ms.

Usually on this type of missions the order of magnitude of the best performances that can be reached when using passive isolators only set at the base of typically 3 wheels is about $1\mu\text{rad}$ for wheel rates varying from 0 to typically 6000 rpm; the major contributors are roughly in the 10Hz to 100Hz range; performances below 10Hz are usually better than $0.1\mu\text{rad}$ thanks to the naturally low wheel disturbances at these frequencies; performances above 100Hz are also generally below $0.1\mu\text{rad}$ thanks to the passive isolator filtering. Note that for the case of Geo-Oculus, passive isolation only is sufficient thanks to wheel rate limitation, but additional operations are required to limit wheels rate.

Hence, in order to meet the $0.1\mu\text{rad}$ micro-vibration global performance objective, the “Active/Passive” solution needs typically to perform a 20dB rejection for disturbances above 10Hz: high frequency perturbations are filtered by the passive isolator, while low frequency ones are rejected by the active control loop.

This active/passive system would be an attractive solution for future high resolution geo-stationary Earth Observation missions.

3 Active /Passive Solution and Test Set-Up Description

Abstract One of the objectives of the study was to assess the performances of the active/passive solution on a real hardware. The hardware developed in the frame of this study can be divided into two parts: the active/passive solution itself, and the test-set-up representative of a satellite panel in free-free conditions. The overall mechanical structure state-space model required for controller synthesis has been obtained and validated thanks to a dedicated MIMO ARMAX-based identification procedure.

3.1 Active Isolation System

The active/passive isolation system hardware developed in the frame of this study is made of the following parts:

- a 4 elastomer-based isolator module
- a set of 4 tri-axis Kistler force sensors connected to charge amplifiers
- 6 WILCOXON proof mass actuators (PMA) to create a 6-DOF torsor, each actuator being connected to a current amplifier
- an active plate on top of the isolator module supports the disturbance source and the 6 PMA
- a control electronics based on a dSpace AUTOBOX driven by a standard PC.

The active controller is modeled and tuned on a PC under SIMULINK. This model is then auto-coded via Real-Time Workshop (RTW), and the corresponding executable is loaded and executed in real-time on the AUTOBOX. The executable running on the AUTOBOX processor provides a control signal vector $u(t)$ to the 6 current amplifiers which convert it into currents towards each PMA; each PMA generates a linear force to its interface with the active plate. The total forces and torques, sum of the forces and torques generated by the PMA and by the disturbance source are transmitted through the active plate and isolator module mechanical structures and measured by the 4 tri-axes force cells; their charges, converted into volts by the charge amplifiers, form the measurement vector $y(t)$ of the controller.

3.2 Test Set-Up description

The test set-up used to assess the performances of the active/passive solution consists in a honeycomb rectangular interface surrounded by 4 metallic beams simulating a satellite panel supporting the active/passive system. The breadboard is suspended by 4 springs in order to reproduce the free-free limit conditions of a satellite in orbit. The disturbance source set on the active/passive isolation system active plate can be either a wheel or a shaker set on a dummy wheel.

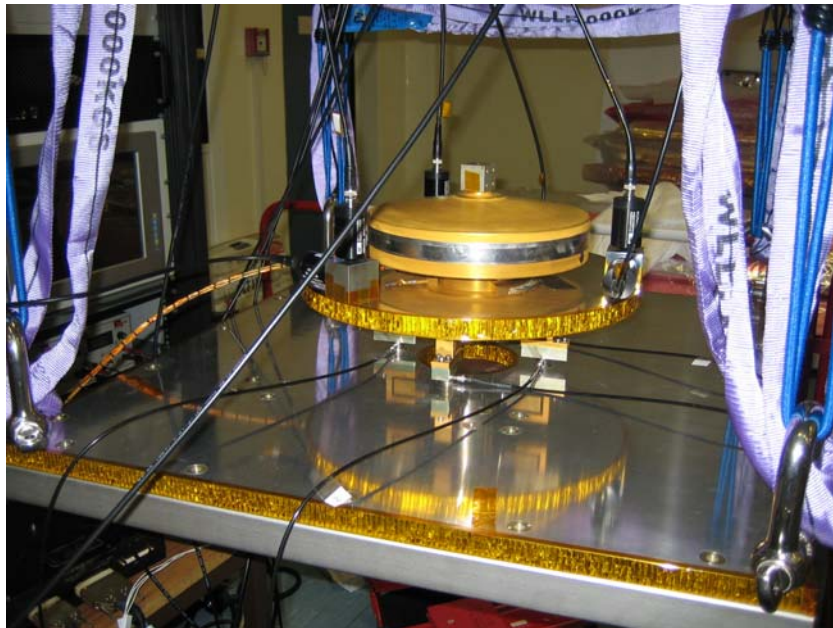


Figure 3.1 The complete breadboard made of the test set-up, the active/passive solution and the disturbance source (here it is a wheel) set on the active plate.

3.3 Structure Identification

The dynamical model with as inputs: the control signals sent to the current amplifiers that drive the PMAs $u(t)$ and as outputs: the measurements provided by the charge amplifiers connected to the force cells $y(t)$, is required by the design and tuning of the active control laws. To elaborate this model, a real-time identification has been performed through a dedicated test. The principle of this identification procedure consists in injecting a 6-axis uncorrelated random noise sequence $u(t)$ to the current amplifiers and to measure the transmitted noise measured by the force cells $y(t)$. Then an ARMAX-based MIMO procedure is applied on these input and output samples to get the linear coefficients of the difference equation linking the expected output vector $\underline{y}(t_n)$ wrt previous measurements $y(t_{n-k})$, wrt current and previous inputs $u(t_{n-k})$ and wrt previous error terms $w(t_{n-k}) = \underline{y}(t_{n-k}) - y(t_{n-k})$. These coefficients are then converted into a state-space representation of the model linking input $u(t)$ to output $y(t)$. Hence the identified plant takes into account all mechanic and electronics that are present on the path from input $u(t)$ to output $y(t)$.

The validation of this structure identification procedure is two-folds: first, one compares the modeled plant output $\underline{y}(t)$ when stimulated by the input noise $u(t)$ used during the experimentation with the real measurements $y(t)$; secondly, one compares the identified modes frequencies to the modes computed by a NASTRAN modal analysis of the system. The NASTRAN model had some limitations. Hence, additional modes were identified: they are due to the springs and to the PMAs modes which were not modeled in NASTRAN. Moreover, one could notice a reduction of the isolator frequencies due to an increase of the inertia itself as the modelization of the PMAs was missing. Uncertainty on modeled modes frequencies was below 5%.

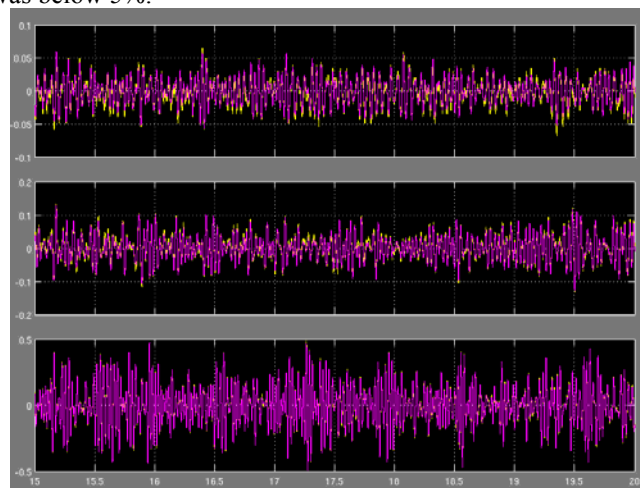


Figure 3.2 Comparison between measurement and identification

4 Active Control Laws

Abstract Two control strategies have been developed: the first one, called anti-phase control, is based on an adaptive feed-forward disturbance cancellation scheme; the second one is a robust stability and performance strategy formulated within the μ -synthesis framework.

4.1 Anti-Phase Cancellation

The principle of this controller basically consists in generating a sinusoidal signal at the same frequency and amplitude as the measured disturbance but with an opposite sign i.e. with a phase equal to the disturbance signal phase $+ 180^\circ$.

The disturbance frequency is deduced from the wheel rate which is supposed to be measured: it is equal to the wheel rate multiplied by the harmonic rank that needs to be cancelled. During the study, harmonic of rank 1 (H1) due to wheel unbalance, and harmonic of rank 0.6 (H0.6) due to wheel cage harmonic were taken into account simultaneously.

The amplitude and phase of the disturbance signal are compensated simultaneously online through a demodulation / re-modulation process: the disturbance signal is first demodulated by multiplication with two unitary amplitude reference sinusoidal signals with a frequency equal to the disturbance frequency, and with a relative 90° phase difference. High frequency components of these products are rejected using low pass filters. The remaining very low frequency components of the products are then sent to a very low bandwidth controller and re-modulated with the reference sine and cosine signals: the resulting signal is sent to the current amplifiers. The very low bandwidth controller consists in a simple proportional / integrator followed by a multiplication with the inverse of the plant matrix linking force cells sensor and current amplifiers at the disturbance frequency. This plant matrix comes from the identification structure procedure.

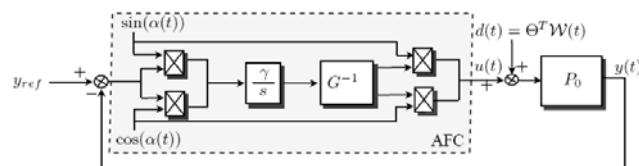


Figure 4.1 Adaptive Disturbance Cancellation scheme also called anti-phase controller

4.2 Robust control design

This second type of controller handles explicitly robust stability and performance objectives during the synthesis procedure. The goal consists in designing a controller stabilizing the closed loop system over a wide range of operating conditions, plant un-modeled dynamics and uncertainties, while robustly satisfying disturbance rejection requirement over a wide frequency range.

Robust design has been executed according to an incremental approach starting with the design of a set of N controllers, each controller being designed and tuned to reject a sinusoidal disturbance at a fixed frequency. The goal of this first step is to investigate the dependence between the robust controllers and the disturbance frequency to derive guideline for the gain scheduling.

The control design has been formulated as a μ -synthesis problem using weighting functions in order to take into account the robust performance and stability requirements. The plant identified during the structure identification process, is considered as the nominal one. The μ -synthesis is based on an uncertain system extracted from a set of several dynamics evaluated by considering 5% uncertainties around the modal frequencies of the nominal plant; the principle consists in finding a controller stabilizing the system despite the considered plant uncertainties while minimizing the closed loop transfer between the disturbance input and the performance signals, in the H_∞ norm sense. Weighting functions are shaped in order to reach at least 6dB gain / 30° phase stability margins, to take into account actuators limitations and to avoid their saturation, and to get 20dB disturbances rejection at the disturbance frequency. The rejection performed by the tuned controller is equivalent to a notch type filter around the disturbance frequency.

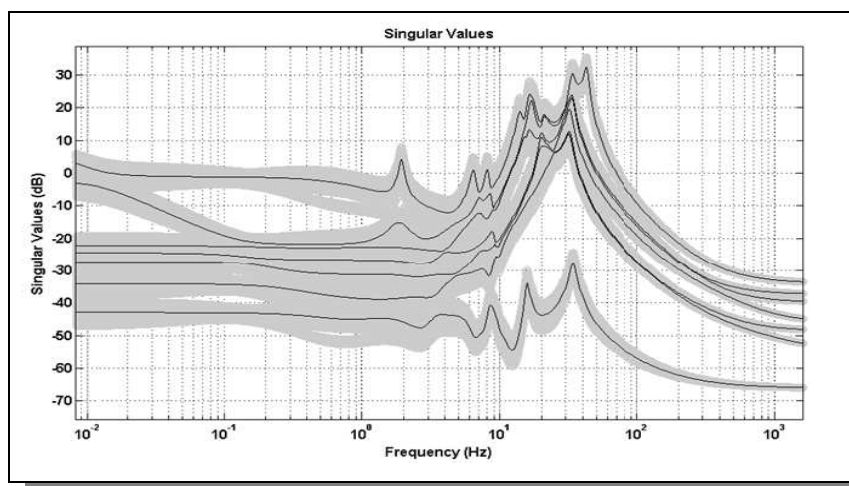


Figure 4.2 Family of uncertain plant dynamics around the nominal one extracted from the identification procedure

12

Ten controllers have thus been designed, each controller being tuned to reject one frequency at respectively 16 Hz, 18, 20, ... and 34 Hz. The resulting stability margins are better than 6.5dB, the rejection level at the disturbance frequency is 20dB, and reaches 0dB (no rejection and no attenuation) for frequencies at ± 2 Hz around the disturbance frequency.

Finally, a controller has been designed to reject simultaneously H1 and H0.6 harmonics of a disturbance with a fundamental frequency equal to 30.5Hz.

4.3 Gain-scheduling control

A gain-scheduling control using the 10 previously synthesized controller has been developed in order to reject any disturbance variation continuously in the [15Hz, 22Hz] frequencies range. This controller is then adapted online wrt the measured disturbance frequency.

5 Performances with Hardware in the Loop

Abstract The two control solutions have been implemented on the hardware test bench and evaluated through a representative performances assessment campaign. The results highlighted the effectiveness of the proposed mixed active/passive isolation strategy and suggest that the robust control solution is a reliable and practical candidate for future space programs.

Performances assessment has been split into steady-state nominal and steady-state robust performances where the disturbance frequency is constant and time-varying performances where the disturbance frequency varies continuously between 15Hz and 22Hz. In tests related to steady-state nominal performances the plant and the disturbance frequencies are supposed to be perfectly known, whereas in tests related to steady-state robust performances the impact of plant uncertainties and of disturbance frequencies knowledge errors on the control performances are assessed.

All performance plots presented below show the force cell measurements projected into the 6-DOF tursor space (3 forces, 3 torques) wrt time. The closed loop responses of the system for the two controllers are superimposed on the same plot.

The test sequence is as follow: first the system is working in open-loop with no disturbance and no control up to $t=20s$. Then, a few seconds later, the disturbance is switched on (shaker on the dummy wheel). Then, a few seconds later, the control is switched-on. About 2 minutes later (e.g. at about $t=140s$), the control is switched-off and then some seconds later the disturbance is switched-off.

5.1 Steady-state nominal performances

In this case, the disturbance frequency and the plant dynamics are supposed to be perfectly known meaning that the controllers have been synthesized on the identified dynamic. Ten frequencies between 16Hz and 34Hz have been tested, but only results at 16Hz and at 32Hz are presented here.

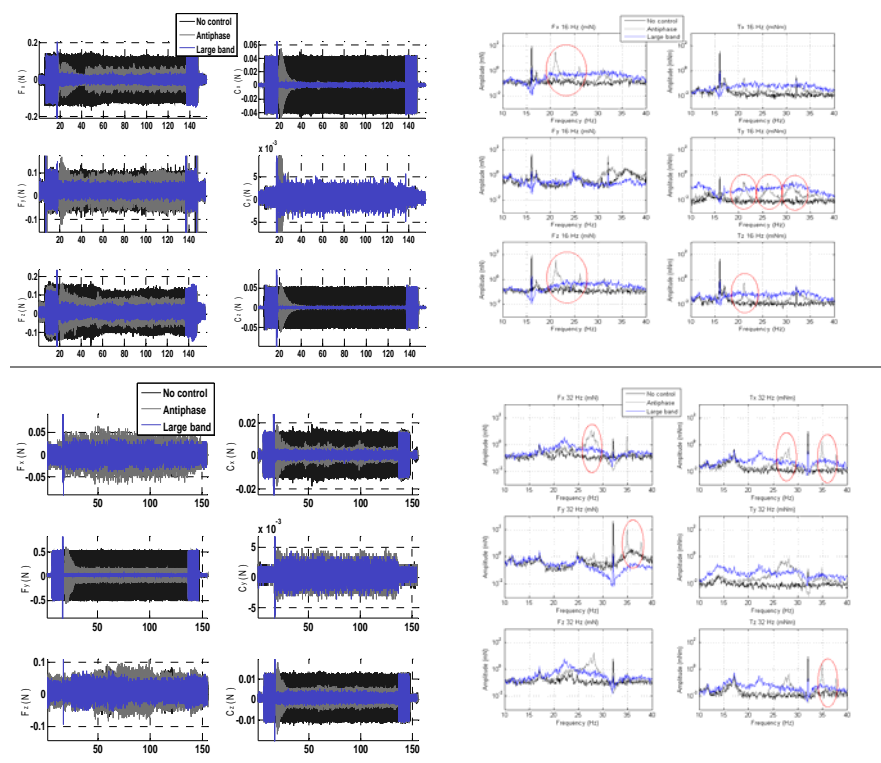


Figure 5.1 Measured forces and torques for disturbance frequency at 16Hz (top) and at 32Hz (bottom), in the time domain (left) and in the frequency domain (right). Anti-phase controller generates some artifacts at frequencies different from the control frequency (see ellipses)

On the above plots, one can notice that transient time is equal to 1s for robust control whereas it is equal to 20s for anti-phase control. Disturbance rejection at the control frequency is comprised between 20dB and 50dB for the robust controller and between 30dB and 60dB for anti-phase controller. Rejection of axial torque (T_y) is better than 8dB only but disturbance amplitude along this axis at the control frequency is two orders of magnitude lower than along the two other torques axis. Anti-phase control generates some artifacts at frequencies different from the control frequency inducing a degradation of its global performance by up to 6dB wrt the robust controller one.

5.2 Steady-state robust performances

Two kind of robustness are addressed: robustness to disturbance frequency knowledge and robustness to plant uncertainty.

A disturbance frequency knowledge error of 0.5Hz has been injected. The plots below show that the anti-phase controller is not able to reject the disturbance, whereas the robust controller rejects the disturbance with a performance comprised between 6dB and 20dB (except for the very low disturbance axis T_y where the performance is close to 0dB but where the disturbance is very low as seen in the steady-state nominal case).

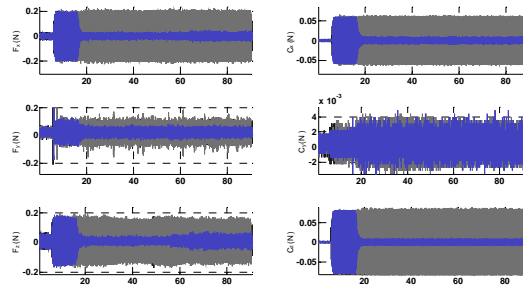


Figure 5.2 Measured Forces and Torques for an error of 0.5Hz on the disturbance frequency

Plant uncertainty has been simulated by synthesizing the controllers with a modification of the identified plant modes frequencies (1-Hz shift). As seen on the plots below, both controllers present good robustness to plant uncertainties with rejection performances at the disturbance frequency comprised between 17dB and 60dB for anti-phase control and between 20dB and 90dB for robust control. Robust control generates artifact at its control frequency: the ratio between the disturbance at 32Hz and these artifacts at 33Hz is comprised between 7dB and 33dB (except for T_y axis where the performance is degraded but where the disturbance is two orders of magnitude lower compared to the other 2 torque axis)

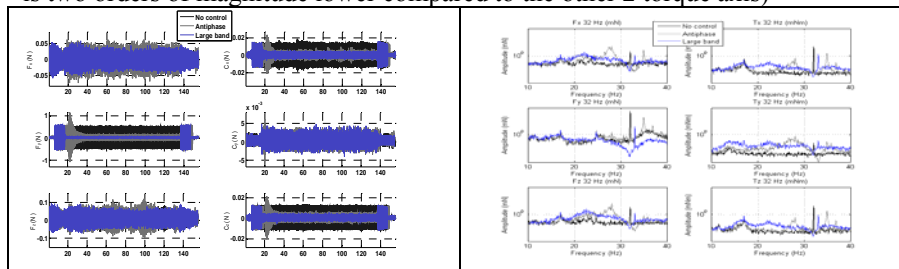


Figure 5.3 Measured Forces/Torques for disturbance frequency at 32Hz with an uncertainty on plant dynamics equal to 1Hz.

5.3 Time-varying performances

During these tests, the disturbance frequency varies continuously wrt time from 15Hz to 22Hz. As it can be seen on the plots below, the performance at the disturbance frequency is comprised between 20dB and 45dB for the anti-phase controller and between 25dB and 30dB for the robust controller, except for T_y where the disturbance is two order of magnitude lower than along the two other torque axis. Some artifacts at 150s can be observed for the anti-phase one.

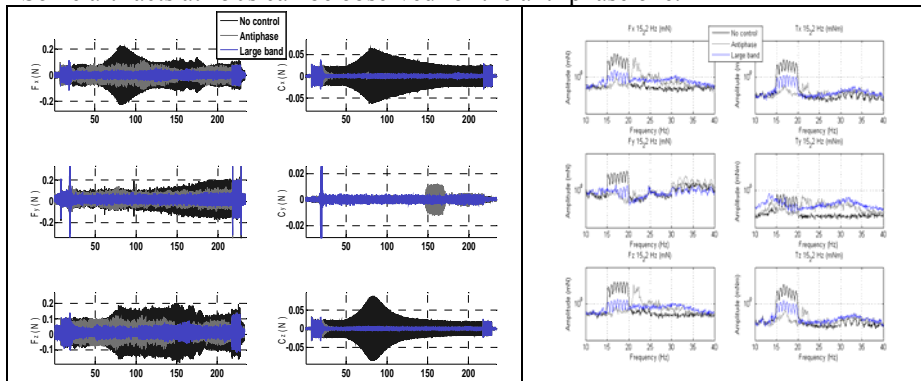


Figure 5.4 Measured Forces and Torques with a continuous variation of the disturbance frequency between 15Hz and 22Hz, with Anti-phase and robust gain scheduling controllers

6 Study conclusions and way-forward

Abstract The performances of active-passive vibration isolation demonstrated during this study on real hardware show that these solutions can significantly enhance the pointing stability of future very high resolution science and observation missions. A subsystem implementing this hybrid active/passive solution would be a very interesting alternative to vibration-free micro-propulsion systems, in terms of cost, mass, and operational complexity thanks to the possibility to use the wheels during the mission phases. The next steps would be the development of further optimized Engineering Model, with flight compatible actuators and a first prototype of the local control electronics.

The hybrid active / passive solution investigated during the study couples elastomer-based passive isolator efficient at high frequency with an active PMA-based control system implementing two types of controllers to reject vibrations at lower frequencies. The first controller is based on anti-phase disturbance cancellation scheme, while the second one is formulated and managed in the μ -setting providing robust stability and robust performances. The robust controller has been extended to provide a gain-scheduling control. The model of the plant, required by the two controller synthesis, has been derived from prior ARMAX-type MIMO identification procedure based on input/output data collected on the real breadboard and including sensors, actuators, structure and electronics. Finally, the two control strategies have been implemented and tested on a real hardware also developed in the frame of the study. The performance campaign revealed the superiority of the robust control solution over the anti-phase one in terms of performances and robustness issues, and demonstrated a robust 20dB rejection at the disturbance frequency.

A subsystem implementing this hybrid active/passive solution can be set at the base of any harmonic disturbance source such as wheels, cryocoolers or control momentum gyros, wheels being the more challenging ones because of the variations of its harmonics frequencies that may interact with structure modes. For missions requiring very high pointing stability performances in the 30 to 100nrad range, such system is a very interesting alternative to micro-propulsion systems, in terms of cost, mass, and operational complexity thanks to the possibility to use the wheels during the mission phases.

The next steps would be the development of further optimized Engineering Model, with flight compatible actuators, and a first prototype of the local control electronics.